Probing the Conformation of the Sugar Transport Inhibitor Phlorizin by 2D-NMR, Molecular Dynamics Studies, and Pharmacophore Analysis

Susanne Wielert-Badt, Jiann-Trzuo Lin, Mike Lorenz, Stefan Fritz,† and Rolf K.-H. Kinne*

Abteilung Epithelphysiologie, Max-Planck-Institut für molekulare Physiologie, Postfach 50 02 47, 44202 Dortmund, Germany

Received November 1, 1999

Sodium/D-glucose cotransport, one of the prototypes for sodium gradient-driven symport systems in kidney and intestine, is known to be inhibited by aromatic and aliphatic glucosides (Diedrich, D. F. *Biochim. Biophys. Acta* **1963**, *71*, 688−700; Diedrich, D. F. *Arch. Biochem. Biophys.* **1966**, *117*, 248−256; Kipp, H.; et al. *Biochim. Biophys. Acta* **1996**, *1282*, 124−130; Ramaswamy, K.; et al. *Biochim. Biophys. Acta* **1976**, *433*, 32−38). The conformation in which the most potent inhibitor, phlorizin, interacts with the transport protein was investigated with different approaches. Phlorizin consists of the glucose moiety and two aromatic rings (A and B) joined by an alkyl spacer. First the interaction of these various parts of the molecule was determined by two-dimensional (2D) solution NMR. From the 2D-NOESY (nuclear Overhauser effect) measurements spatial distances (up to 5 Å) between various interacting H atoms could be detected. Using these values as distance constraints, conformations of phlorizin were calculated and analyzed by the valence force-field method. As a result, a set of conformations could be obtained. The most probable phlorizin conformation shows a nearly perpendicular arrangement of the two aromatic rings (A and B) with the ring B situated above the sugar ring. A very similar conformation could be found by using molecular dynamics simulations when water was chosen as the solvent. This phlorizin conformation in aqueous solution then served as a template for conformational analysis of various phlorizin derivatives. The resulting conformations of derivatives were taken as input to establish a pharmacophore model using the DISCO calculation. As a result, the essential elements of phlorizin for interaction with its binding pocket could be deduced: namely hydrogen bonding via hydroxyl groups of the pyranoside at C_2, C_3, C_4, and C_6 and at C_4 and C_6 of aromatic ring A and hydrophobic interactions via the pyranoside ring and aromatic ring A. Finally, from these conformational features of the pharmacophore the dimension of the phlorizin binding site on the sodium/D-glucose cotransporter was estimated to be 17 × 10 × 7 Å^3.

Introduction

D-Glucose transport across luminal membranes of the cells in the renal proximal tubule and small intestine is mediated by Na^+/D-glucose cotransporter. These cotransport systems are inhibited by glucosides with either aromatic or aliphatic aglucone residues.[1−6] Phlorizin, a β-glucoside of the aromatic compound phloretin, is the most potent inhibitor among the known glucosides with an apparent K_i value of 1 μM.[2,7] The Na^+/D-glucose cotransporter is an intrinsic membrane protein with 14 transmembrane spans[8] and 662 amino acids.[9,10] Despite extensive studies the location and molecular nature of the binding/translocation sites for D-glucose and/or phlorizin are still unknown. A direct approach to solve this question could be affinity labeling with the subsequent characterization of the labeled sites and/or crystallization of the cotransporter in the absence and presence of glucose or phlorizin. However, realization of these approaches to date is still hampered by the lack of sufficient amounts of pure cotransporter and the complex nature of membrane proteins. An indirect way to approximate the interactions between a substrate and/or inhibitor and the cotransporter is to determine the conformation of phlorizin in solution and subject the data on various derivatives to pharmacophore analysis.[11]

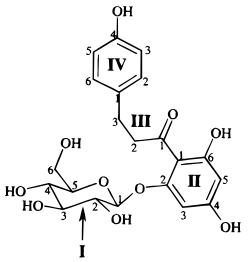

Figure 1. Chemical structure of phlorizin, subdivided into four segments: I, pyranoside ring; II, aromatic ring A; III, connecting alkyl chain and carbonyl group; IV, aromatic ring IV.

The conformation of phlorizin in a crystallized state has been solved. According to those studies the molecules exhibit an extended coplanar arrangement of the two aromatic rings II and IV[12] (Figure 1). But because the pharmacologically active concentrations of phlorizin are much lower than the concentrations used during crystallization the question remains whether this conformation reflects the biologically active form that interacts with the transporter. In addition, a model was developed by Diedrich from the relative inhibitory potency of various analogues[2] and a conformation was

* Corresponding author. Phone: +49-231-133 22 01. Fax: +49-231-133 22 99. E-mail: rolf.kinne@mpi-dortmund.mpg.de.
† Present address: Adolf-Butenandt-Institut für Physiologische Chemie I, Goethestr. 33, 80336 München, Germany.

10.1021/jm9905460 CCC: $19.00
Published on Web 04/18/2000

suggested, based on molecular mechanics calculation using the Tripos force field in vacuo.[13] However, the former model was purely speculative, and in the latter the conformational analysis was performed in vacuo, an approach that overestimates *intramolecular* interactions due to omission of solvent molecules. Bearing these limitations in mind, we therefore reanalyzed the conformation of phlorizin using parameters that mimic the physiological conditions more closely.

The initial studies involved NMR utilizing NOESY (nuclear Overhauser enhancement exchange spectroscopy) which is one of the most direct ways to determine spatial distances between two interacting H atoms within a molecule in the range up to 3−5 Å.[14] Hereafter molecular modeling using the constraints established by the NMR studies followed. Both methods predicted that the relative positions of the aromatic ring II and pyranoside ring position were similar to that found in the crystal but that the relative position of aromatic ring IV differed considerably. This conformation of phlorizin was then used as a template for the analysis of phlorizin derivatives and employed as input to generate a pharmacophore map for phlorizin. Such pharmacophore maps can provide valuable insight not only into receptor−ligand interactions[11,15,16] but also into the three-dimensional shape of binding pockets in proteins.[13,17,18] Thus, the size of the binding pocket of the Na^+/D-glucose cotransporter for phlorizin could be estimated and the interactions between the inhibitor and the transporter could be specified.

Materials and Methods

Materials. All chemicals used were of the highest purity available. Phlorizin was obtained from Sigma (Deisenhofen, Germany). For NMR studies phlorizin was either dissolved directly in 50 mM phosphate buffer to give a 2 mM solution or a 1 M stock solution in DMSO was diluted in a 50 mM Na_2HPO_4 buffer (pH 7.4) to yield a final concentration of 0.1 M.

Methods. 1. NMR Spectroscopy. All one- and two-dimensional NMR spectra were recorded with a Bruker Avance DRX 500 (11.7 T) at temperatures from 278 to 318 K (Bruker, Karlsruhe, Germany). Two-dimensional NOESY was recorded with 4 K data points and 512 tracks to define the spatial interactions between protons based on the appearing cross-peaks. Prepulses of the solvent frequency or a gradient field achieved suppression of the water signal. The mixing time of the 2D-experiments was 300 ms. Chemical shifts are given in δ values with TMS or TSP as internal standard. The spectra were processed with the XWIN NMR program, version 1.2 (Bruker). 2D spectra were analyzed with the program NMR-Triad of SYBYL (Tripos, St. Louis, MO).

2. Computer-Aided Modeling. All calculations were performed on a Silicon Graphics Indy workstation. The analysis was based on molecular mechanics[19,20] using the Tripos force-field calculation[21,22] as implemented in SYBYL (v. 6.2). The charges were calculated using the Gasteiger and Hückel method.[23,24]

A: Analysis of Phlorizin Conformation Using the Constraints Obtained from NMR Studies. The resulting cross-peaks of the 2D-NOESY experiments were converted into proton−proton distances using MardiGras and Generating Constraints (programs Exact and Range) modules of SYBYL.[25,26] At first, the relaxed crystal structure of phlorizin was taken as the starting structure and complemented with the addition of proton−proton distances as intramolecular constraints. The conformational search of the whole molecule was carried out using the random search algorithms[27] with variation of all torsion angles between segments I and IV (see below). To ensure a complete search, at least 7000 runs with subsequent minimization were performed. The minimization process was done according to the methods of Powell.[28] The conformation attributed with the lowest energy represents the most favorable for each set of constraints. The low-energy conformations (up to 15 kcal/mol above the minimum energy structure) of the different distance constraints sets were compared.

B: Molecular Dynamics Simulations. Similar to the conformation analysis, the relaxed crystal structure of phlorizin was taken, to use the pyranoside as a rigid template for the molecular dynamics simulations. In the molecular dynamics simulations the trajectory of phlorizin was recorded, which is the conformation as a function of time by integration of the Newton equation of motion (see eq 1) of all atoms of the system:

$$m_i \frac{\partial^2 x(t)}{\partial t^2} = m_i a_i(t) = \vec{F}_i = -\vec{\nabla}_i E \qquad (1)$$

with m_i = mass, $x(t)$ = position, F_i = force on atom i, and E = potential energy of the system.

For each integration step small time intervals of typically 1−10 fs were chosen.[29] The whole simulation was carried out over a period of 250 or 600 ps with conformation snapshots every 500 fs.[29] For the simulation in H_2O, $CHCl_3$ or CH_3CN, respectively, phlorizin was solvated using the droplet-solvation method of SYBYL, where a specified amount of solvent layers is gradually put around the solvate.[30] A short minimization (100 steps simplex, 100 steps Powell minimization) of the complex was added to reduce unfavorable solvent-phlorizin contacts.[31] The dynamics simulation was carried out with periodic boundary conditions that implied a constant solvent concentration and a constant temperature resulting in a canonical ensemble.[31] From the resulting set of conformations the statistic equilibrium values could be determined by averaging over the whole trajectory[31] for each solvent.

3. Generation of Phlorizin Pharmacophore. A: Conformation Analysis of Phlorizin Derivatives. The molecular models of the phlorizin analogues (Table 3) were built based on the phlorizin conformation obtained from the NMR study. The conformational analysis was carried out as described above using random search algorithms[27] with variation of the torsion angles between segments II and IV and the additional substituents listed in Table 3. Afterward, conformations of each phlorizin analogue with energy lower than 15 kcal/mol above the global energy minimum (cutoff range) were selected, and the respective conformations were stored in a separate database for each derivative. The optimized conformations of all inhibitors were superposed on the phlorizin molecule.

For evaluation of the correlation between conformation and biological activity, the inhibition constants K_i of phlorizin analogues for the Na^+/D-glucose cotransport determined by Diedrich, Vick et al., Hahn, and Wielert-Badt et al.[5,32−34] were used. The estimates of the affinity of the transporter for the reference compound phlorizin in these studies are close enough so that a direct comparison appears to be justified.

B: Generation of the Pharmacophore. The DISCO module (DIStance COmparison)[11] of SYBYL was used to calculate the pharmacophoric map of phlorizin and its derivatives. Conformations of all phlorizin derivatives with the lowest energy content (after conformational analysis) were first aligned to phlorizin representing the reference conformation. For each conformation, the possible pharmacophoric elements, i.e., the points to be considered as part of the superposition, were assigned. These are, for example, atoms in the molecules (hydrogen-bond donors and acceptors, charged groups, aromatic and aliphatic ring systems) and projections from the ligands to hydrogen-bond donors and acceptors or charged groups in the binding site. The search program uses a click-detection method to find superpositions that contain at least one conformation of each molecule containing user-specified numbers of elements (e.g. hydrogen-bond acceptors or donors) and chirality. Different runs using varied numbers and types of elements were executed. The distances between the elements in each 3D conformation of derivatives were calculated

Table 1. Cross-Peaks from 2D-NOESY Experiments with Phlorizin[a]

spatial interaction between	no.	cross-peak between	proton−proton distance: crystal structure (Å)	MardiGras (Å)	Exact (Å)	Range (Å)
I and II	1	I1−II3	4.7	2.57	2.50	2.25−2.87
	2	I5−II3	3.3	2.82−2.83	2.77	2.49−3.18
I and IV	3	I1−IV2,6	2.6/6.6	4.89/5.05	3.78	3.40−4.34
III and IV	4	III2−IV2,6	2.4	3.58−3.60	2.74	2.46−3.14
	5	III2−IV2,6	4.7	3.83−3.85	3.27	2.91−3.75
	6	III3−IV2,6	2.7	3.74−3.76	3.18	2.86−3.65

[a] Segments and atoms indicated as in Figure 1; proton-proton distances calculated with MardiGras, Exact, and Range modules of SYBYL.

and added to the reference table (phlorizin). The intramolecular distances of identical elements between the reference conformation and the calculated conformations of derivatives were compared. The significance of distance difference was initially set to 0.5 Å and distances were considered to be identical if the distance was smaller than this value and the atom types were identical. If the previously specified elements such as number of hydrogen-bond acceptors and donors, hydrophobic elements and chirality were met within this distance significance, a valid pharmacophoric map was established. If no solution with the specified criteria was found the distance tolerance was increased (distance tolerance set stepwise from 0.5 to 5 Å) and the calculations were repeated.[11]

Results and Discussion

NMR Analysis and Determination of Spatial Proton−Proton Distances. For clarity, phlorizin can be subdivided into four fragments based on structural properties (Figure 1): the pyranoside with hexose structure (segment I), the polyphenoxyl aromatic ring (segment II), the alkyl chain (segment III) containing a carbonyl group, which links the two aromatic rings, and the phenoxyl aromatic ring (segment IV). The NOESY spectrum of phlorizin obtained at 310 K shows six cross-peaks with various intensities (see Supporting Information for details). The cross-peaks are listed in Table 1. Interactions occur between segments I and II (I1−II3, I5−II3), segments I and IV (I1−IV2, I1−IV6), and segments III and IV (III2−IV2, III2−IV6, III3−IV6). There was no temperature-dependent change in number and size of cross-peaks when spectra were recorded from 5 to 45 °C indicating stable intramolecular spatial interactions between the respective atoms. From the integrals of the NOESY signals resulting from the cross-peaks the respective proton−proton distances were calculated using the modules MardiGras, Exact, and Range of Triad, SYBYL. The calculated distances are also listed in Table 1. The program MardiGras thereby predicts a more relaxed conformation compared to the other two. The distances between the pyranoside ring and the aromatic ring II (I1−II3 and I5−II3) and between the pyranoside ring and the aromatic ring IV (I1−IV2 and I1−IV6) are key information for the conformation in aqueous solution. No cross-peaks were detected for the interactions between the two aromatic rings, suggesting that a "stacked" conformation of phlorizin as calculated previously in vacuo (see below) was not likely.

Conformational Analysis Using Distance Constraints. Using the estimated distances as constraints, the analysis should reflect the statistically valid conformation in solution. The conformation found in the crystal was used as the starting structure for conformation analysis using the random search algorithm. The calculated intramolecular distances obtained in all three programs as shown in Table 1 were separately applied to the phlorizin molecule as distance constraints.

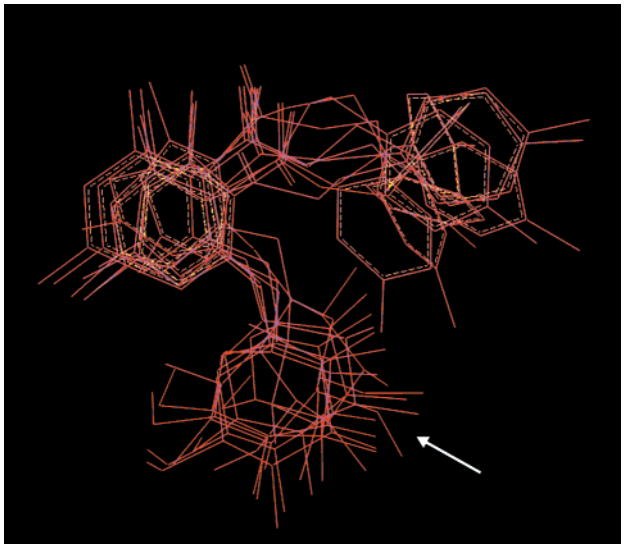

Figure 2. Phlorizin conformations obtained by random search analysis using the distance constraints derived from NMR data. Sugar moiety indicated by an arrow. Only the conformations with a minimum energy ≤ 15 kcal/mol are shown.

Using distance constraints determined with the three different modules Exact, Range, and MardiGras, different numbers of conformation were found: 18, 20, and 28 conformations, respectively. When only those sets of conformations with energy content up to 15 kcal/mol above minimum energy were assembled, the conformations obtained using the three different models (with different distance constraint values) were virtually identical. The root-mean-square (rms) deviation was found to be 1.39 ± 0.22 Å for all conformations generated. These selected low-energy conformations are displayed in Figure 2 with the sugar moiety indicated by an arrow.

Comparing these conformations with the existing models, first the proposal by Diedrich[2] will be considered. Diedrich postulates a phlorizin conformation from the differences of inhibitory potential of various analogues with an intramolecular hydrogen bond between the hydroxyl group at C6 of segment I and the carbonyl group of segment III, resulting in a coplanar arrangement of the glucoside and the aromatic ring II precisely oriented with respect to the remainder of the molecule. However, no rotation in the connecting alkyl chain of segment III was considered. The existence of a hydrogen bond between segment I OH6 and the CO group of segment III is not excluded by the NOESY spectra of phlorizin obtained in the current studies. Nevertheless, as this configuration was not contained in the set of conformations obtained after random search with applied distance constraints, it was no longer considered as potential phlorizin conformation in solution.

The conformation most frequently found with all three models of distance constraints was chosen (Figure 3, middle) and used as a reference for the subsequent studies. The torsion angles of this conformation are listed in Table 2, line 1. This conformation was similar

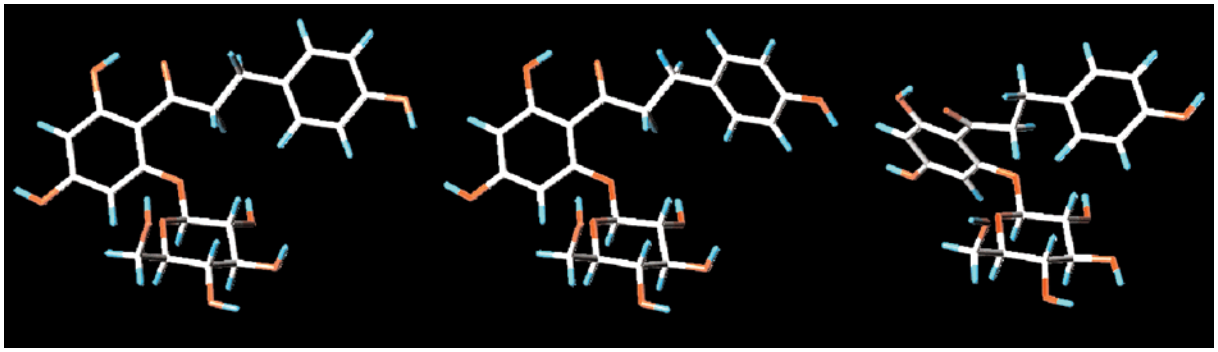

Figure 3. 3D structures of phlorizin: crystal structure (left), conformation after NMR study (middle), conformation after molecular dynamics simulation in H_2O (right); white − carbon atoms, blue − hydrogen atoms, red − oxygen atoms.

Table 2. Comparison of Phlorizin Conformation from NMR Data and Averaged Phlorizin Conformations from Molecular Dynamics Simulations in Water[a]

no.	phlorizin	period (ps)	I1−II1 (deg)	II1−III1 (deg)	III1−III2 (deg)	III2−III3 (deg)	III3−IV2 (deg)	III3−IV6 (deg)
1	NMR data		154.8	18.5	148.0	158.7	73.5	−105.7
	MD							
2	in H_2O	250	110.2	21.2	135.0	175.5	97.9	−82.1
3	in H_2O	600	117.4	14.3	125.9	180.0	91.1	−89.2
4	crystal structure		159.2	−1.6	−179.2	−178.1	175.0	−5.0

[a] Torsion angles between assigned segments (I−IV) were determined after 250 and 600 ps, respectively. The arabic indices denote the position of atoms from which the values of torsion angles were given.

to the one found in the crystal (Figure 3, left) with respect to the relative position of the pyranoside and the aromatic ring II. The most striking difference was that the aromatic ring IV was twisted about 100° in aqueous solution compared to the coplanar arrangement in the crystal. This difference in conformation is understandable when considering the different conditions applied for NMR studies and crystallization. At high phlorizin concentrations, similar to those used for crystallization, a graphite-like *inter*molecular interaction between the aromatic rings of adjacent phlorizin molecules could occur. This could restrict the freedom of rotation of aromatic ring IV and lead to a coplanar alignment of the aromatic rings. In aqueous solution, particularly at the micromolar concentrations of phlorizin used in binding and inhibition studies, the molecule is likely to be present as a monomer and *intra*molecular interactions between the individual parts of a single molecule rather than *inter*molecular interactions between several molecules would prevail. Therefore, to establish the conformation a single phlorizin molecule might assume molecular dynamics simulations were performed.

Molecular Dynamics Simulations of Phlorizin Conformations. Molecular dynamics simulations were performed over a period of 250 or 600 ps with steps of 1 fs. From the resulting set of conformations the statistic equilibrium values were determined by averaging over the whole trajectory. The prolonged simulation of phlorizin in water for 600 ps, for example, did not show any additional conformations and also no alteration of any dominating conformations.

The conformation of phlorizin after molecular dynamics simulation in H_2O (Figure 3, right) was again only partly identical to that found in the crystal. In agreement with the previous NMR studies but contrary to the conformation in the crystal, aromatic ring IV was tilted about 90° out of the plane of the phlorizin molecule. Simulations carried out in more hydrophobic solvents such as chloroform and acetonitrile were designed to see whether the conformation would change in a more hydrophobic environment. Due to the overall conformational identity indicated by small rms deviations between the conformations generated in the different solvents, changes in the hydrophobicity of the phlorizin environment do not seem to be a major determinant of the conformation. Therefore, only the conformation from the molecular dynamics calculations in water was further considered.

If the torsion angles derived from the NMR studies (number 1, Table 2) are compared with those calculated in water (numbers 2 and 3, Table 2) and those present in the crystal (number 4, Table 2), it can clearly be seen that the values between those based on the NMR studies and those calculated in water are similar throughout the entire phlorizin structure, whereas the conformation in the crystal is strikingly different for most parts of the aglucone moiety but not for the pyranoside ring. Thus, the molecular dynamics calculation independently confirmed the conformation in water predicted from the NMR study. These studies using low phlorizin concentrations appear to be more reliable to determine a relevant conformation for the interaction of phlorizin with the cotransporter; therefore the latter was used as reference for further studies concerning the conformational analysis of inhibitory phlorizin analogues as the first step for the calculation of the pharmacophore model.

Conformational Analysis of Inhibitory Phlorizin Analogues. Since, as demonstrated above, the conformation based on the constraints obtained from NOESY measurements was virtually identical to that calculated by molecular dynamics calculations in water, it was used as the starting point for the analysis of inhibitory phlorizin analogues which are listed together with their K_i values in Table 3. All conformations found by random search of the torsion angles in the substituent groups and subsequent energy minimization of each inhibitor were compared and the low-energy conformations were selected and stored in separate databases. The number

Table 3. Phlorizin Derivatives Used for Creating the Phlorizin Pharmacophore[a]

no.	inhibitor	K_i (μM)	I2	I3	II4	IV3	IV4	no. of conformers
1	phlorizin	0.18[33]	OH	OH	OH	H	OH	2
2	4′-deoxyphlorizin	0.56[33]	OH	OH	H	H	OH	3
3	phloretin 2′-(2-deoxyglucoside)	2.60	H	OH	OH	H	OH	3
4	4-methoxyphlorizin	2.80[33]	OH	OH	OH	H	OCH_3	3
5	3-aminophlorizin	3.80[34]	OH	OH	OH	NH_2	OH	6
6	3-*p*-nitrobenzylideneaminophlorizin	5.30[34]	OH	OH	OH	NCHPh-6-NO_2	OH	13
7	3-iodoacetamidophlorizin	7.00	OH	OH	OH	$NHCOCH_2I$	OH	11
8	3-bromoacetamidophlorizin	7.70[34]	OH	OH	OH	$NHCOCH_2Br$	OH	12
9	phloretin 2′-galactoside	14.0[33]	OH	OH	OH	H	OH	3
10	3-nitrophlorizin	21.6[34]	OH	OH	OH	NO_2	OH	3
11	3,5,5′-tribromophlorizin	23.1[34]	OH	OH	OH	Br	OH	3
12	3′-iodo-3-iodoacetamidophlorizin	40.0	OH	OH	OH	$NHCOCH_2I$	OH	11
13	phloretin 2′-(3-methoxyglucoside)	45.0[33]	OH	OCH_3	OH	H	OH	3
14	3,5,3′,5′-tetrabromophlorizin	93.1[34]	OH	OH	OH	Br	OH	3
15	3-dansylphlorizin	94.3[34]	OH	OH	OH	$NHSO_2$naph-5-$N(CH_3)_2$	OH	4
16	3-succinamidophlorizin	116.0[34]	OH	OH	OH	$NHCOCH_2CH_2COOH$	OH	5
17	3-amino-6-sulfophlorizin	152.0[34]	OH	OH	OH	NH_2, SO_3H	OH	6
18	phlorizin chalcone	>1000[33]	OH	OH	OH	H	OH	3
19	phloretin	86.0[33]	OH	OH	OH	H	OH	-

[a] All inhibitors are classified as the parent compound, phlorizin (Figure 1); positions and types of substituents are indicated. The inhibitory constants K_i to phlorizin binding were either from published data or measured in isolated renal brush border membranes. All derivatives were analyzed by constrained random search using the established phlorizin conformation as template (see Materials and Methods). Conformers with energy content < 15 kcal/mol were used as input for DISCO analysis; the number of conformers for each analogue is listed.

Table 4. Specified Criteria for Calculation of Pharmacophoric Models Using DISCO (SYBYL): Number of Elements To Be Found in DISCO Runs within Certain Distance Tolerance To Yield a Pharmacophoric Model[a]

	run 1	run 2	run 3	run 4	run 5	run 6	run 7
no. of acceptor atoms	>5[b]	>4	>3	>3	>4	>4	>3
donor atoms	>5	>4	>3	>3	>4	>4	>3
hydrophobic rings	>2	>2	>2	>1	>1	>0	>1
acceptor sites	na[c]	na	na	na	na	>1	>1
donor sites	na	na	na	na	na	>1	>1
range of distance tolerance, DT (Å)	0.5−5	0.5−5	0.5−5	0.5−5	0.5−5	0.5−5	0.5−5
step size (Å)	0.5	0.5	0.5	0.5	0.5	0.5	1
mismatch	all[c]	all	all	all	all	all	all
pharmacophore model with DT < 5 Å				1, 2	3		4−7

[a] If no model was found with a demanded number of elements within distance tolerance, the required number of elements was reduced in following runs. Details of resulting pharmacophore models in Table 5. [b] Figures denote number for each assigned element to meet during each run. [c] na, not assigned; nall, not allowed; all, allowed.

Table 5. Pharmacophore Models Resulting from Calculation with DISCO (SYBYL): Pharmacophoric Elements of All Phlorizin Analogues, Distance Tolerance for All Pharmacophoric Elements in All Derivatives, and Excluded Derivatives of the Respective Model[a]

calculated pharmacophoric elements	pharmacophore model						
	1	2	3	4	5	6	7
acceptor atoms	I: O1, O3, O4, O5 II: O4, O6	I: O2, O3, O4, O5 II: O6	I: O2, O3, O4, O6 II: O4, O6	I: O2, O4	I: O2, O4	I: O2, O5	I: O3, O5, O6
donor atoms	I: O3, O4 II: O4, O6	I: O2, O3, O4 II: O4, O6	I: O2, O3, O4, O6 II: O4, O6	I: O2, O4	I: O2, O4	I: O2	I: O3, O6
acceptor sites				I: O3, O3*H*	I: O3, O3*H*, O4	I: O2, O2*H*	I: O3, O4
donor sites				I: O3, O3*H*, O5	I: O3, O3*H*, O4	I: O2, O2*H*	I: O3, O4
hydrophobic elements	sugar moiety aromatic ring II	sugar moiety aromatic ring II	sugar moiety aromatic ring II	sugar moiety	sugar moiety	sugar moiety	sugar moiety
tolerance limit (Å)	1.0	1.0	1.0	1.0	1.0	1.0	1.0
excluded derivatives	phloretin 2′-(3-methoxy-glucoside) phloretin 2′-galactoside	phloretin 2′-(3-methoxy-glucoside) 2-deoxyphlorizin	phloretin 2′-(3-methoxy-glucoside) 2-deoxyphlorizin	2-deoxy-phlorizin	2-deoxy-phlorizin	2-deoxy-phlorizin	none

[a] Segment I = glucose moiety, segment II = aromatic ring A according to Figure 1.

of potential low-energy conformations for each derivative used for generating the pharmacophore map are listed in Table 3 as well.

Generation of the Pharmacophore. To generate the pharmacophore, phlorizin served as the reference to which all conformations of each analogue were aligned. After assignment of possible pharmacophoric elements for each analogue (see Materials and Methods) the calculation and analysis were carried out using the DISCO program and a superposition of molecules, including the assigned elements, was attempted. Several runs of calculation were repeated to generate pharmacophore maps. For each run a distinct number of specified pharmacophoric elements as listed in Table 4 (runs 1−7) was adapted. The analysis resulted in only a few models where all pharmacophoric elements were

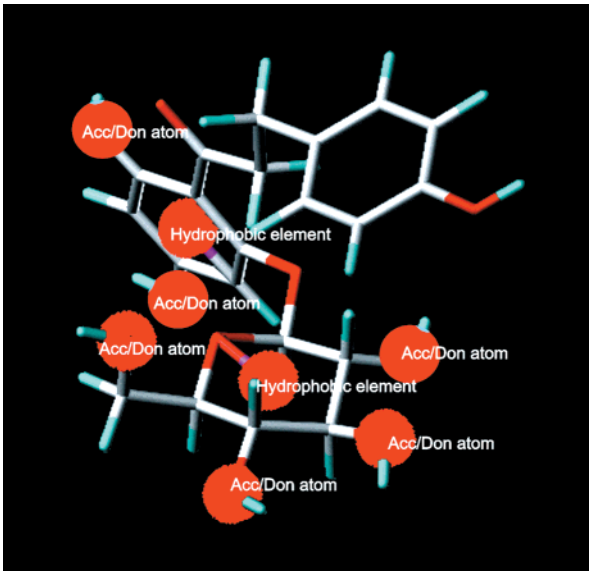

Figure 4. Pharmacophore model 3: white − carbon atoms, blue − hydrogen atoms, red − oxygen atoms, red spheres − pharmacophoric elements of model 3.

within a distance tolerance of maximal 5 Å. In some cases, where no solution within the distance tolerance could be found (Table 4, runs 1−3, 6), a reduction of the number of elements followed by recalculation was carried out to generate a new pharmacophoric set. The elements of the pharmacophore models obtained under these circumstances with the corresponding distance tolerances are listed in Table 5. All models showed that the donor and acceptor atoms of the sugar hydroxyl groups and the sugar moiety as hydrophobic element were well superimposed within the set distance tolerance. This confirms the important role of the sugar moiety for recognition and binding of the phlorizin derivatives to the Na^+/D-glucose cotransporter.

Models 1−3 possess pharmacophoric elements in the pyranoside as well as in the aglucone moiety. In contrast, models 4−7 showed common elements only in the pyranoside moiety. Since the aglucone part of phlorizin plays an important role in binding,[1,2] models 4−7 were excluded from further considerations. For selection between models 1 and 3, an additional criterion was needed. Based on the binding studies,[1,2,33] the OH groups at positions 2, 3, 4, and 6 are crucial for binding. Furthermore it is rather unlikely that the ring oxygen atom O5 is involved in hydrogen bonding. As shown in Table 5, in pharmacophore model 3, only O2, O3, O4, and O6 are involved in hydrogen bonding whereas in models 1 and 2 the sugar ring oxygen atom O5 was assigned the unprobable role of an acceptor atom for hydrogen bonding. Therefore, model 3 was considered as the representative pharmacophore map of the phlorizin inhibitors fitting the phlorizin binding pocket of the cotransporter as displayed in Figure 4. The respective intramolecular distances of the pharmacophore elements are provided as Supporting Information.

In conclusion, the conformation of phlorizin probably relevant for its interactions with the cotransporter derived from the current studies is quite different from those described previously. The phlorizin conformation proposed by Lostao et al.[13] was derived by variation of torsion angles of 20−60° per bond in vacuo which is quite different from our conformational analysis. In preliminary studies there were clear indications that conformational analysis performed in vacuo yielded a remarkably different global energy minimum with a conformation where the aromatic ring IV folded back over the aromatic ring II to yield a sandwich-like arrangement (S. Wielert-Badt, unpublished results). However, as we now applied intensive random search considering experimentally determined distance constraints (the sandwich-like structure is just out of the detection limit of cross-peaks) and molecular dynamics simulations using a solvated system for conformational analysis, the current study can be considered to yield more reliable data about the phlorizin conformation in a physiological environment.

According to model 3, the interactions via hydrogen bonds from the 2-, 3-, 4-, and 6-hydroxyl groups of the pyranoside and the 4- and 6-OH groups of the aromatic ring II are essential for phlorizin binding.

One interesting fact that needs to be addressed is the aromatic ring IV: as a result of the pharmacophore analysis, the elements selected from the aromatic ring IV were all outside of the required distance tolerance limit, i.e., 5 Å. In other words, the ring probably lies, at least partly, in the periphery of the binding pocket.

From the conformational information of the resulting pharmacophore model 3 (Figure 4) dimensions of the phlorizin recognition/binding pocket could be estimated. Measuring the distances between the van der Waals radii of atom O4 in segment II to atom O4 in IV, between the radii of atom H3 in segment I to atom H2 in segment IV, and between O6 of segment I to O2 in segment I, the size of the phlorizin binding pocket was estimated to be 13 × 10 × 17 $Å^3$. This is larger than the dimensions of the SGLT1 substrate (D-glucose) transport pocket given by Panayotova-Heiermann et al.[35] with 10 × 5 × 5 $Å^3$. The difference between the glucose transport pocket and the phlorizin recognition pocket is probably due to the different probes used for the estimation. In the former studies, arbutin,[13] a monophenoxyl glucoside and almost linear and extremely flexible molecule, was used that can be translocated across the membrane by the cotransporter. In contrast, in our studies, phlorizin, a glucoside containing two aromatic rings, which is not translocated across the brush border membrane[36] was employed. Thus, a larger area of interaction would be expected.

Further studies including affinity labeling experiments are in progress in our laboratories to define the regions of the SGLT molecules that interact with phlorizin and hopefully will pave the way to direct structure−activity relationship studies.

Acknowledgment. We thank B. Griewel for expert technical support and assistance in the NMR measurements and Dr. F. Schmitz for assistance in application of SYBYL programs. The excellent editorial and secretarial work of Daniela Mägdefessel is also gratefully acknowledged.

Supporting Information Available: NOESY spectrum of phlorizin in phosphate buffer and a table of the calculated intramolecular distances between the 2-OH group of the sugar moiety and the other pharmacophoric elements of phlorizin. This material is available free of charge via the Internet at http://pubs.acs.org.

References

(1) Diedrich, D. F. The comparative effects of some phlorizin analogues on the renal reabsorption of glucose. *Biochim. Biophys. Acta* **1963**, *71*, 688−700.

(2) Diedrich, D. F. Competitive inhibition of intestinal glucose transport by phlorizin analogues. *Arch. Biochem. Biophys.* **1966**, *117*, 248−256.

(3) Kipp, H.; Lin, J. T.; Kinne, R. K. H. Interactions of alkylglucosides with the renal sodium/D-glucose cotransporter. *Biochim. Biophys. Acta* **1996**, *1282*, 124−130.

(4) Ramaswamy, K.; Bhattacharyya, B. R.; Crane, R. K. Studies on the transport of aliphatic glucosides by hamster small intestine in vitro. *Biochim. Biophys. Acta* **1976**, *433*, 32−38.

(5) Silverman, M. Structure and function of hexose transporters. *Annu. Rev. Biochem.* **1991**, *60*, 757−794.

(6) Wright, E. M. The intestinal Na^+/glucose cotransporter. *Annu. Rev. Physiol.* **1993**, *55*, 575−589.

(7) Kinne, R. K. H. Properties of the glucose transport system in the renal brush border membrane. *Curr. Top. Membr. Transp.* **1976**, *8*, 209−267.

(8) Turk, E.; Kerner, C. J.; Lostao, M. P.; Wright, E. M. Membrane topology of the human Na^+/glucose cotransporter SGLT1. *J. Biol. Chem.* **1996**, *271*, 1925−1934.

(9) Hediger, M. A.; Coady, M. J.; Ikeda, T. S.; Wright, E. M. Expression cloning and cDNA sequencing of the Na^+/glucose cotransporter. *Nature* **1987**, *330*, 379−381.

(10) Kanai, Y.; Lee, W. S.; You, G.; Brown, D.; Hediger, M. A. The human kidney low affinity Na^+/glucose cotransporter SGLT2. *J. Clin. Invest.* **1994**, *93*, 397−404.

(11) Martin, Y. C. M.; Bures, M. G.; Danaher, E. A.; DeLazzer, J.; Lico, I.; Pavlik, P. A. A fast new approach to pharmacophore mapping and its application to dopaminergic and benzodiazepine agonists. *J. CAMD* **1993**, *7*, 83−102.

(12) Auf'mKolk, M.; Köhrle, J.; Hesch, R.-D.; Ingbar, S. H.; Cody, V. Crystal structure of phlorizin and the iodothyronine deiodinase inhibitory activity of phlorizin analogues. *Biochem. Pharmacol.* **1986**, *35*, 2221−2227.

(13) Lostao, M. P.; Hirayama, B. A.; Loo, D. D. F.; Wright, E. M. Phenylglucosides and the Na^+/glucose cotransporter (SGLT1): Analysis of interactions. *J. Membr. Biol.* **1994**, *142*, 161−170.

(14) Friebolin, H. *Ein- und zweidimensionale NMR−Spektroskopie*; VHC: Weinheim, 1988; p 239.

(15) Myers, A. M.; Charifson, P. S.; Owens, C. E.; Kula, N. S.; McPhail, A. T.; Baldessarini, R. J.; Booth, R. G.; Wyrick, S. D. Conformational analysis, pharmacophore identification, and comparative molecular field analysis of ligands for the neuromodulatory 3 receptor. *J. Med. Chem.* **1994**, *37*, 4109−4117.

(16) Spadoni, G.; Balsami, C.; Diamantini, G.; Di Giacomo, B.; Tarzia, G. Conformationally restrained melatonin analogues: synthesis, binding affinity for the melatonin receptor, evaluation of the biological activity, and molecular modeling study. *J. Med. Chem.* **1997**, *40*, 1990−2002.

(17) Minor, D. L.; Wyrick, S. D.; Charifson, P. S.; Watts, V. J.; Nichols, D. E.; Mailman, R. B. Synthesis and molecular modeling of 1-phenyl-1,2,3,4-tetra-hydroisoquinolines and related 5,6,8,9-tetrahydry-13b*H*-dibenzo[a,*h*]quinoli-zines as D1 Dopamine antagonists. *J. Med. Chem.* **1994**, *37*, 4317−4328.

(18) Waller, C. L.; Wyrick, S. D.; Kemp, W. E.; Park, J. M.; Smith, F. T. Conformational analysis, molecular modeling, and quantitative structure−activity relationship studies of agents for the inhibition of astrocytic chloride transport. *Pharm. Res.* **1994**, *11*, 47−53.

(19) Boyd, D. B.; Lipkowitz, K. B. Molecular mechanics − the method and its underlying philosophy. *J. Chem. Educ.* **1982**, *59*, 269−272.

(20) Cox, P. J. Molecular mechanics − illustration of its applications. *J. Chem. Educ.* **1982**, *59*, 275−277.

(21) Clark, M.; Cramer III, R. D.; Van Opdenbosch, N. Validation of the general purpose Tripos 5.2 force field. *J. Comput. Chem.* **1989**, *10*, 982−1012.

(22) Motoc, I.; Dammkoehler, R. A.; Mayer, D.; Labanowski, J. Three-dimensional quantitative structure−activity relationships. I. General approach to the pharmacophore model validation. *Quant. Struct.-Act. Relat.* **1986**, *5*, 99−105.

(23) Gasteiger, J.; Marsili, M. Iterative partial equalization of orbital electronegativity − a rapid access to atomic charges. *Tetrahedron* **1980**, *36*, 3219−3228.

(24) Purcell, W. P.; Singer, J. A. A brief review and table of semiempirical parameters used in the Hueckel molecular orbital method. *J. Chem. Eng. Data* **1967**, *12*, 235−246.

(25) *MardiGras, TRIAD2 release notes 7/95, SYBYL V.6.2*; Tripos: St. Louis, MO, 1995; Chapter 8.

(26) *Generating Constraints, TRIAD2 release notes 7/95, SYBYL V.6.2*; Tripos: St. Louis, MO, 1995; Chapter 7.

(27) Saunders: M.; Houk, K. N.; Wu, J. D.; Still, W. C.; Lipton, M.; Chang, G.; Guida, W. C. Conformation of cycloheptadecane. A comparison of methods for conformational searching. *J. Am. Chem. Soc.* **1990**, *112*, 1419−1427.

(28) Powell, M. J. D. Restart procedures for the conjugate gradient method. *Mathematical Programming* **1977**, *12*, 241−254.

(29) van Gunsteren, W. F.; Berendsen, H. J. C. Moleküldynamik-Computersimulationen; Methodik, Anwendungen und Perspektiven in der Chemie. *Angew. Chem.* **1990**, *102*, 1020−1055.

(30) *SYBYL V.6.2, theory manual, droplet solvation*; Tripos: St. Louis, MO, 1995.

(31) Kunz, R. W. *Molecular Modelling für Anwender*; Teubner Verlag: Stuttgart, Germany, 1991.

(32) Wielert-Badt, S.; Kinne, R. K.-H., Lin, J.-T. 3-Iodoacetamidophlorizin and 3′-iodo-3-iodoacetamidophlorizin as affinity label for the Na^+/D-glucose cotransporter (SGLT1). *Anal. Biochem.*, submitted.

(33) Vick, H.; Diedrich, D. F.; Baumann, K. Reevaluation of renal tubular glucose transport inhibition by phlorizin analogues. *Am. J. Physiol.* **1973**, *224*, 552−557.

(34) Hahn, K. D. Untersuchungen zur Substratspezifität des Glukosecarriers in Nierenzellmembranen. Ph.D. Thesis, Frankfurt am Main, Germany, 1980.

(35) Panayotova-Heiermann, M.; Loo, D. D. F.; Kong, C. T.; Lever, J. E.; Wright, E. M. Sugar binding to Na^+/glucose cotransporters is determined by the carboxyl-terminal half of the protein. *J. Biol. Chem.* **1996**, *271*, 10029−10034.

(36) Toggenburger, G.; Kessler, M.; Semenza, G. Phlorizin as a probe of the small-intestinal Na^+, D-glucose cotransporter. A model. *Biochim. Biophys. Acta*, **1995**, *688*, 557−571.

JM9905460